



ELSEVIER

Microelectronics Journal 39 (2008) 485–488

---



---

**Microelectronics  
Journal**


---



---

www.elsevier.com/locate/mejo

# Bandstructure and photoluminescence of SiGe islands with controlled Ge concentration

M. Brehm<sup>a</sup>, T. Suzuki<sup>a</sup>, Z. Zhong<sup>a,b</sup>, T. Fromherz<sup>a,\*</sup>, J. Stangl<sup>a</sup>, G. Hesser<sup>a</sup>, S. Birner<sup>c,d</sup>,  
F. Schäffler<sup>a</sup>, G. Bauer<sup>a</sup>

<sup>a</sup>*Institute for Semiconductor and Solid State Physics, University Linz, Austria*

<sup>b</sup>*Physics Department, Fudan University, 200433 Shanghai, China*

<sup>c</sup>*Walter Schottky Institute, Technical University Munich, D-85748 Garching, Germany*

<sup>d</sup>*Nextnano<sup>3</sup>, Frauenmantelanger 21, D-80937 Munich, Germany*

Available online 11 September 2007

---

## Abstract

The dependence of the photoluminescence (PL) emission wavelength of SiGe islands embedded into a Si matrix on their Ge concentration and gradient was investigated. Intense PL signals at wavelengths that can be shifted over most of the telecom wavelength range (1.38–1.77  $\mu\text{m}$ ) by varying the Ge concentration were observed. Using the structural island parameters determined by AFM, TEM, and a careful analysis of X-ray reciprocal space maps, good agreement between calculated and measured PL emission wavelength was achieved, indicating that by combining PL and X-ray experiments, an accurate determination of the Ge concentration and a quantitative modeling of the bandstructure of the SiGe islands is possible.

© 2007 Elsevier Ltd. All rights reserved.

**Keywords:** SiGe islands; Photoluminescence; Bandstructure calculations

---

## 1. Introduction

Due to its indirect fundamental bandgap in  $k$ -space, bulk silicon—the dominating material for microelectronics—is not suitable for optoelectronic applications. Nevertheless, the demand for processing and transmitting a large amount of data in very short times is steadily increasing, and intra-chip optical communication links will become more and more important in the near future [1]. Evidently, a Si-based optoelectronic platform compatible with modern CMOS technology is highly desirable. Promising sources for light emission in the SiGe system are quantum dots (QDs). It is well known [2] that due to the strain field originating from the QDs, not only holes, but also electrons are bound to the QDs. Due to this confinement, the  $k$ -space selection rules are relaxed in all three dimensions. However, while the holes are bound to the Ge-rich region in the interior of the

QDs, the electrons are localized in the Si matrix along the surface of the QDs. Thus, a spatial indirect (type II) band alignment results [2] and optical interband matrix elements are expected to be small. For optimizing the emission efficiency, a detailed understanding of the bandstructure and its dependence on the structural parameters of the SiGe dots are a prerequisite. In this work, we focused on the influence of the Ge content and its gradient along the growth axis on the emission wavelength and efficiency.

Samples containing a single layer of SiGe QD were grown by solid source MBE. For the Si buffer and QD layer, a growth temperature (rate) of 650 °C (1 Å/s) was used. On top of the buffer, a SiGe alloy layer with the target Ge concentration  $x_b$  for the base of the QD was deposited. The Ge flux was kept constant until 3D island nucleation was observed in the RHEED pattern and then ramped up/down in order to reach the desired Ge concentration  $x_t$  at the top of the QD. After QD growth, part of the wafer was covered by a shutter during the growth of the 150 nm Si capping layer. The capping layer growth started with a growth temperature (rate) of 450 °C

---

\*Corresponding author. Altenbergerstrasse 69, University of Linz, A-4040 Linz, Austria. Tel.: +43 732 2468 9602; fax: +43 732 2468 8650.

E-mail address: [Thomas.fromherz@jku.at](mailto:Thomas.fromherz@jku.at) (T. Fromherz).

(0.5 Å/s) and was ramped up after 10 nm to 650 °C (1 Å/s). TEM, AFM, and X-ray diffraction were used to investigate the structural parameters of the SiGe islands. These parameters served as input for calculating the bandstructure of the islands by the nextnano<sup>3</sup> code [3]. From the bandstructure, the emission energy of the islands is calculated and compared to the photoluminescence (PL) spectrum measured at 6 K under excitation with an Ar-ion laser at a wavelength of 514 nm and an intensity of 5 W/cm<sup>2</sup>.

## 2. Results and discussion

The part of the sample covered with a shutter during capping layer growth was used for measuring the dimensions of the QDs by AFM. Paraboloidal islands with base radii and heights between 70–150 and 12–60 nm, respectively, as indicated in Fig. 1, are observed depending on  $x_b$  and  $x_t$ . The inter-island distance is typically a few nanometers in these samples. In Fig. 1, the measured PL spectra are shown. For all samples, an intense PL band is observed, the spectral position of which can be adjusted within the telecom range from 0.7 eV (1.77 μm) to 0.9 eV (1.37 μm) by the Ge content of the islands.

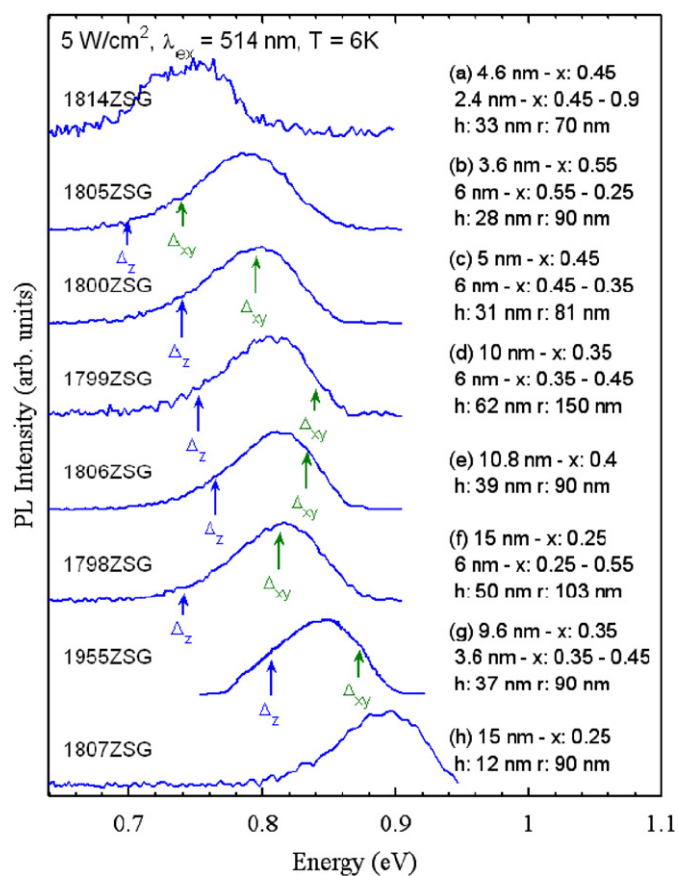


Fig. 1. (Color online) Measured PL spectra for SiGe islands with nominal structural parameters indicated in the plot. The arrows indicate the calculated PL transition energies for the  $\Delta_z \rightarrow \text{HH}$  and  $\Delta_{xy} \rightarrow \text{HH}$  transitions for islands with laterally not overlapping strain fields. The calculations are based on the *nominal* structural parameters.

The samples shown in Fig. 1 were grown with an intentionally varied Ge flux during the growth of the islands resulting in a gradient of the Ge concentration along the growth direction. By establishing this gradient we tried to investigate the influence of the position of the electrons and holes in their respective ground states on the luminescence efficiency and energy of the samples. As an example, the dependence of the ground state positions on the Ge gradient is shown in Fig. 2a and b for sample 1805. For two different Ge gradients [55–25% (nominal, Fig. 2b) and 36–50% (Fig. 2a)], the ground state wavefunctions for the electrons and holes as calculated by nextnano<sup>3</sup> are shown in a 3D isosurface plot. Here, the red, green, and blue surfaces confine the spatial regions, within that the squared moduli of the ground state wavefunctions for the heavy holes (HH), the electrons in the  $\Delta$ -valleys oriented perpendicular ( $\Delta_{xy}$ ) and parallel ( $\Delta_z$ ) to the growth direction, respectively, are larger than 3% of their maximum. For isolated islands, the calculations show that the electron ground state with the lowest energy is the  $\Delta_z$  state. A gradient with more Ge at the base than at the apex localizes the HH ground state at the base (see Fig. 2b), resulting in an unfavorable configuration with vanishing

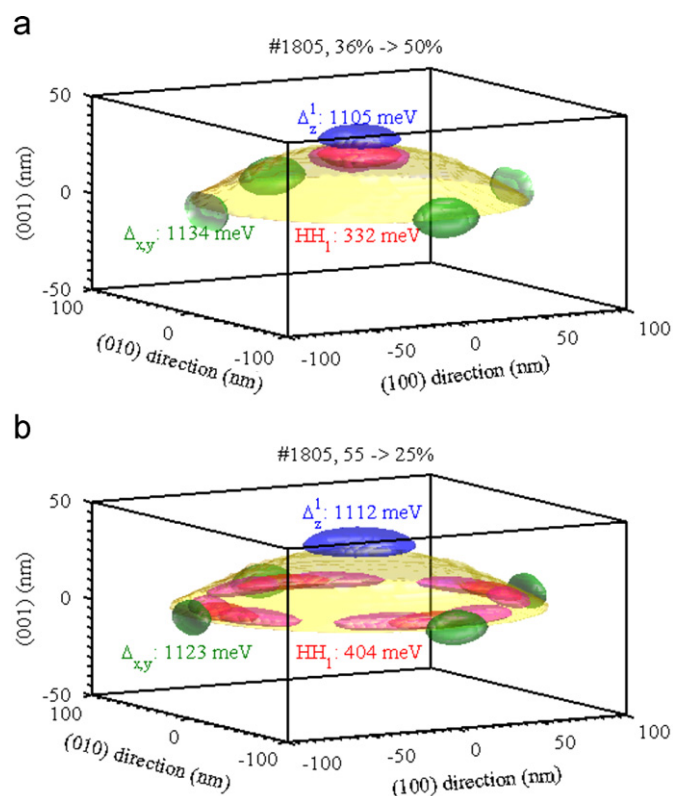


Fig. 2. (Color online) Comparison of the bandstructures of paraboloidal island ( $r$ : 90 nm,  $h$ : 28 nm) for two different linear Ge gradients [(a) 36–50%; (b) 55–25%]. The island surface is shown in yellow, the blue, green, and red surfaces confine the regions in which the squared wavefunction moduli  $|\psi_{\Delta_z}|^2$ ,  $|\psi_{\Delta_{xy}}|^2$ ,  $|\psi_{\text{HH}}|^2$  are larger than 3% of their maximum. The holes are concentrated in the regions of the islands with maximum Ge concentration. The ring-like shape of the HH wavefunction in (b) is caused by the strain in the island.

overlap of the electron and hole ground state wavefunctions. On the other hand, the overlap between the energetically higher lying  $\Delta_{xy}$  states with the heavy hole (HH) ground state is enhanced in this situation, and radiative  $\Delta_{xy}$ -HH recombination seems to be more likely than  $\Delta_z$ -HH recombination, given that the non-radiative lifetime in the  $\Delta_{xy}$  states is large enough for a sufficiently large meta-stable electron population to be established there.

The arrows shown in Fig. 1 indicate the calculated  $\Delta_z$ -HH and  $\Delta_{xy}$ -HH transition energies that were obtained by using the nominal structural parameters in the nextnano<sup>3</sup> calculations. It is evident that for all samples shown in Fig. 1 the calculated energy difference between the  $\Delta_z$ -HH and  $\Delta_{xy}$ -HH transitions is smaller or comparable to the observed inhomogeneously broadened width of the PL emission band. Thus, from comparing these data to the calculated transition energies, it is not possible to identify which transition ( $\Delta_z$ -HH or  $\Delta_{xy}$ -HH) is observed. Most probably, the broadening of the PL emission bands is due to a statistical variation of the island size and distance (the influence of the island distance will be discussed in the following sections).

Also the observed shift of the PL line for the various samples is smaller than the calculations based on the nominal structural island parameters indicate. In order to determine the actual structural parameters, and to check whether the designed Ge gradient was correctly established in our growth process, extensive X-ray experiments were performed. In these experiments, we concentrated on the pair of samples with the largest gradient in opposite directions (#1805 and #1798). X-ray diffraction around the 004 and 224 reciprocal lattice points were performed at the beam line BW2 of Hasylab (Hamburg). For various assumed parameter sets for the Ge gradient and inter-island distance (the island dimensions were determined by AFM and TEM measurements), the strain distribution in the samples was calculated by finite element (FEM) calculations. Using the results of the FEM calculations, the X-ray intensity around the (115) reciprocal space points was calculated and compared to the measured reciprocal space maps. The best agreement between simulated and measured X-ray maps was achieved assuming that the lateral inter-island distance approaches zero. Under this assumption, for several combinations of  $x_b$  and  $x_t$  equally good agreement between simulated and measured maps can be obtained.

For sample 1805, the range of  $x_t$  and  $x_b$  for that X-ray fits have been performed, is shown on the abscissa of Fig. 3 together with the nominal parameters (left end of axis) that are not compatible with the X-ray data. The gradients shown at the center of the axis result in significantly better fits than the gradients on both ends of the axis. Large deviations from the nominal parameters follow from the X-ray analysis indicating that it is difficult to control the Ge gradient during the island growth. As an example for a good fit, the result of the X-ray simulation for sample #1805 assuming a linear gradient from  $x_b = 40\%$  to

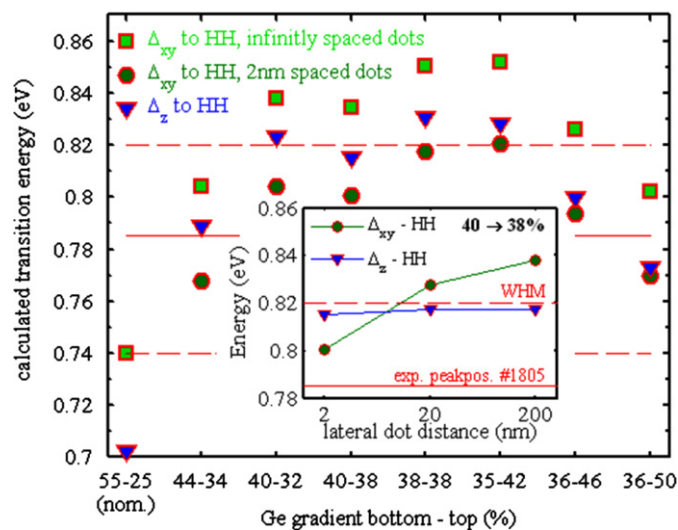


Fig. 3. (Color online) Calculated PL energies using the dimensions of sample 1805 and the Ge gradients indicated on the abscissa. Blue (green) symbols indicate the calculated  $\Delta_z \rightarrow \text{HH}$  ( $\Delta_{xy} \rightarrow \text{HH}$ ) transition energies. Circles (squares) indicate results for 2 nm ( $\infty$ ) spaced islands. Inset: Dependence of the calculated PL energies on the island separation for islands with 40%  $\rightarrow$  38% Ge gradient in more detail. The full (broken) red lines show the measured peak position (FWHM).

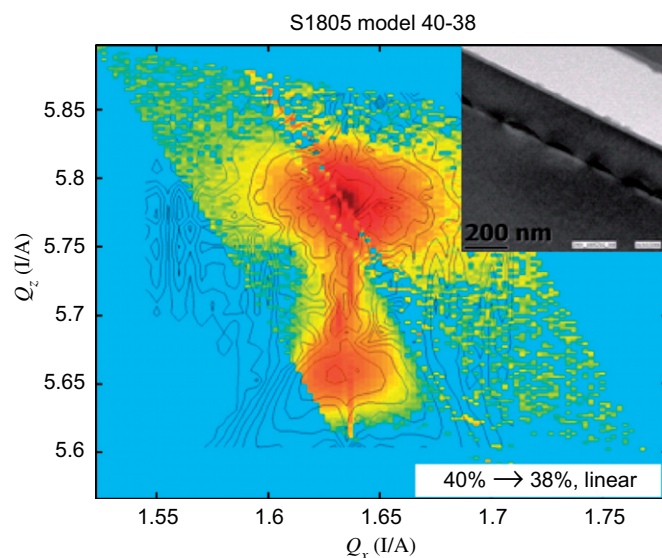


Fig. 4. (Color online) Contour plot of measured (color) and simulated (full lines) X-ray reciprocal space map for sample 1805. The good fit shown was obtained assuming a Ge gradient of 40%  $\rightarrow$  38% and vanishing island spacing. Inset: TEM picture of sample 1805.

$x_t = 38\%$  is shown by the contour lines in Fig. 4 superimposed over the experimental data. For the combinations of  $x_b$  and  $x_t$  shown in Fig. 3, nextnano<sup>3</sup> energy band calculations have been performed. The calculated  $\Delta_{xy}$ -HH and  $\Delta_z$ -HH PL transition energies are shown by the green and blue symbols in Fig. 3. For the  $\Delta_{xy}$ -HH transition, the results for two assumed lateral inter-island distances (infinity, 2 nm) are shown (squares, circles). The calculations show that the  $\Delta_{xy}$ -HH transition energy is sensitive to the inter-dot distance. This is because the

energy of the  $\Delta_{xy}$ -states is determined by the compressive strain in the Si around the base of the island. This energy is lowered if the strain fields of adjacent islands start to overlap. The dependence of the  $\Delta_{xy}$ -HH transition energy on the lateral dot distance is shown in the inset of Fig. 3 for sample #1805 with an assumed Ge gradient of 40–38%. For this sample, the  $\Delta_{xy}$  states become the electron states with the lowest energy at an inter-island distance below  $\sim 10$  nm. The measured energy and FWHM of the PL line observed for sample #1805 are indicated, respectively, by the full and broken red lines in Fig. 3. For an assumed inter-dot distance of 2 nm, good agreement between calculated and measured PL transition energies is obtained for those gradients, for which also the X-ray simulations result in the best fits (40–32%, 40–38%). The other gradients shown in Fig. 3, for which the nextnano<sup>3</sup> results also agree reasonably with the measured PL energy, produce no convincing correspondence between measured and simulated X-ray data.

For sample #1798, a consistent fit of PL energy and X-ray data are obtained assuming a Ge gradient of 31–20%. For this gradient, a  $\Delta_{xy}$ -HH transition energy of 0.83 eV is calculated for 2 nm spaced island, in good agreement with the measured PL peak for this sample as shown in Fig. 1.

### 3. Summary

Intense PL bands are observed for single-layer SiGe islands with intentionally varied Ge content grown by

MBE. Depending on the Ge content, the PL emission wavelength is observed at various wavelengths covering the whole technologically important telecom wavelength range. From both the simulation of X-ray reciprocal space maps and the calculation of PL transition energies based on the nextnano<sup>3</sup> code, the Ge concentration and its gradient within the islands can be determined consistently. The obtained results strongly deviate from the nominal values, indicating that a tight control of the Ge gradient in the islands is a difficult task. In addition to the variation of the island size, the statistical variation of the inter-island distance is identified as a source of inhomogenous PL linebroadening.

### Acknowledgements

This work was supported by the Austrian Science Fonds FWF (SFB IRON, Proj. nos. F2512-N08 and F2507-N08).

### References

- [1] <[http://mph-roadmap.mit.edu/about\\_ctr/report2005/5\\_ctr2005\\_silicon.pdf](http://mph-roadmap.mit.edu/about_ctr/report2005/5_ctr2005_silicon.pdf)>.
- [2] O. Schmidt, K. Eberl, Strain and band-edge alignment in single and multiple layers of self-assembled Ge/Si and GeSi/Si islands, *Phys. Rev. B* 62 (2000) 16715–16720.
- [3] <<http://www.wsi.tu-muenchen.de/nextnano3/index.htm>>.